Third-order and fifth-order nonlinear spin-current generation in *g*-wave and *i*-wave altermagnets and perfectly nonreciprocal spin current in *f*-wave magnets

Motohiko Ezawa
Department of Applied Physics, The University of Tokyo, 7-3-1 Hongo, Tokyo 113-8656, Japan

(Received 26 November 2024; revised 9 February 2025; accepted 7 March 2025; published 26 March 2025)

A prominent feature of d-wave altermagnets is the pure spin current generated in the absence of spin-orbit interactions. In the context of symmetry, there are s-wave, p-wave, d-wave, f-wave, g-wave, and i-wave magnets. In this paper, making an analytic study of two-band Hamiltonian systems coupled with electrons, we demonstrate unexpectedly that only the ℓth order nonlinear transverse spin current proportional to E^ℓ is generated in higher-wave symmetric magnets when the number of nodes is $\ell+1$. Here E is applied electric field. The nonlinear spin current is essential provided the linear spin current is absent. Indeed, only the third-order nonlinear spin current is generated in g-wave altermagnets, while only the fifth-order spin current is generated in i-wave altermagnets. In particular, only the second-order nonlinear spin current is generated in f-wave magnets, which leads to a perfect nonreciprocal spin current. On the other hand, there is no spin-current generation in p-wave magnets.

DOI: 10.1103/PhysRevB.111.125420

I. INTRODUCTION

Pure spin current is a fundamental concept in spintronics, where spin current flows but no charge current flows. It is usually generated by the spin-Hall effect induced by spin-orbit interactions [1–3]. However, the spin-orbit interaction shortens the coherent length of the spin current because it rotates the spin direction. It limits the application of spin current. Recently, it was shown [4–8] that the spin current is generated without the spin-orbit interaction in d-wave altermagnets with the aid of a spin-split band structure. Its coherence length may be longer than that generated by the spin-orbit interaction.

In the context of symmetry, there are s-wave, p-wave [9–11], d-wave [4–9], f-wave [10,11], g-wave [12,13], and i-wave [12,13] magnets which are compatible with the lattice symmetry. We call them higher-wave symmetric magnets. Especially, d-wave, g-wave, and i-wave magnets break time-reversal symmetry and are called altermagnets [12]. However, the problem of spin-current generation still remains to be uncovered in the higher-wave symmetric magnets, except for the d-wave altermagnet.

There are several studies on nonlinear conductivity. Especially, second-order nonlinear conductivity has been extensively investigated [14–28]. The ℓth nonlinear conductivity $\sigma^{a_1a_2\cdots a_\ell;b}$ is defined by $j_b^\ell = \sigma^{a_1a_2\cdots a_\ell;b}E_{a_1}E_{a_2}\cdots E_{a_\ell}$, where E_{a_i} is the applied electric field along the a_i direction, j_b^ℓ is the ℓth nonlinear current along the b direction. Here, some directions can be identical, such as $a_1 = a_2 = \cdots = a_\ell = x$. Nonlinear spin current generation is also interesting [29–32].

In this paper, we study linear and nonlinear spin-current generation in higher-wave symmetric magnets and show that the system has only the ℓth order nonlinear spin-Drude conductivity when the number of the node is $\ell+1$. Note that the linear spin current corresponds to the case of $\ell = 1$. We obtain the following results: There is no spin current generation in s-wave and p-wave magnets. Only the linear spin current is generated in the d-wave altermagnet. The second-order nonlinear spin current is generated in the f-wave magnet, where the current flowing direction is identical irrespective of the direction of applied electric field. The third-order nonlinear spin current is generated in the g-wave altermagnet, while the fifth-order nonlinear spin current is generated in the i-wave altermagnet. These results are summarized in the following table:

	s	p	d	f	g	i
Nodes	0	1	2	3	4	6
ℓ			Linear	Second NL	Third NL	Fifth NL
2D	None	None	$\sigma_{\rm spin}^{y;x}$	$\sigma_{\rm spin}^{xx;y}$	$\sigma_{\rm spin}^{yyy;x}$	$\sigma_{\rm spin}^{yyyyy;x}$
3D	None	None	$\sigma_{\rm spin}^{y;x}$	$\sigma_{\rm spin}^{zy;x}$	$\sigma_{\rm spin}^{xxx;z}$	$\sigma_{\rm spin}^{yyyyx;x}$

II. FERMI SURFACE SYMMETRY

The Fermi surface of electrons coupled with a magnet is known to have the s-wave symmetry as shown in Fig. 1(a). Recently proposed altermagnets generalize it to Fermi surfaces possessing higher-wave symmetries [12,13]. The Fermi surface has 0, 1, 2, 3, 4, and 6 nodes for s-wave, p-wave, d-wave, f-wave, g-wave, and i-wave symmetry, respectively. The d-wave altermagnet has the Fermi surface with d-wave symmetry as shown in Fig. 1(c1). In a similar way, the Fermi surface of the g-wave altermagnet is shown in Fig. 1(e1) and

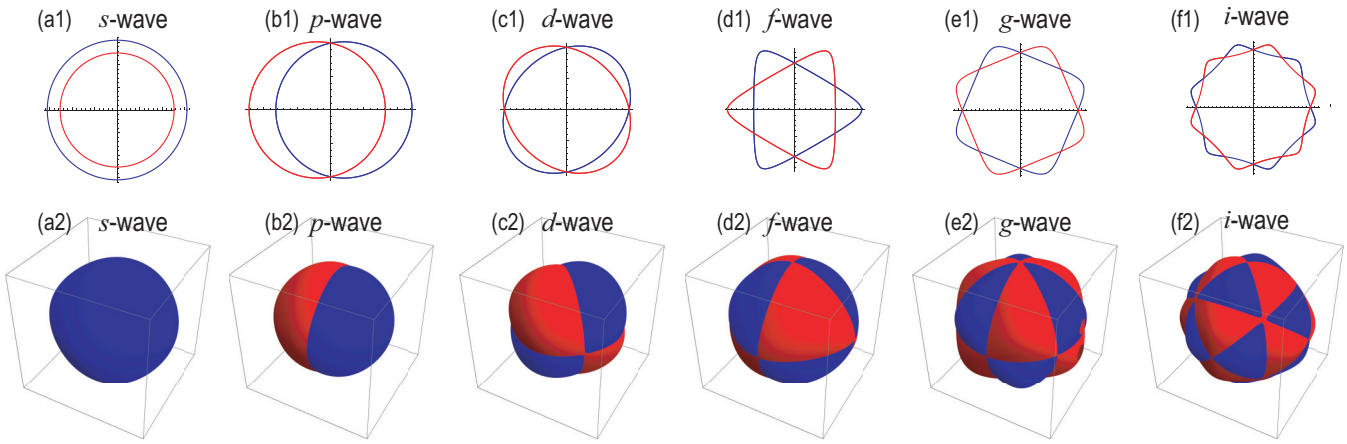

FIG. 1. Fermi surfaces in two and three dimensions. (a1), (a2) s-wave magnet; (b1), (b2) p-wave magnet; (c1), (c2) d-wave magnet; (d1), (d2) f-wave magnet; (e1), (e2) g-wave magnet; (f1) and (f2) i-wave magnet. Red (blue) curves indicate up (down-)-spin Fermi surfaces.

that of the i-wave alatermagnet is shown in Fig. 1(f1). Altermagnets break time-reversal symmetry. On the other hand, p-wave magnets preserve time-reversal symmetry. Its Fermi surface has the p-wave symmetry as shown in Fig. 1(b1). In a similar way, f-wave magnets have Fermi surfaces with the f-wave symmetry as shown in Fig. 1(d1). We note that there are no h-wave magnets because of the incompatibility between the fivefold rotational symmetry and the lattice symmetry. The simplest expressions on magnetic terms with higher symmetries in two dimensions are summarized as follows:

$$H_s^{2D} = J\sigma_z, \tag{1}$$

$$H_p^{2D} = Jk_x\sigma_z, \tag{2}$$

$$H_d^{2D} = Jk_xk_y\sigma_z, \tag{3}$$

$$H_f^{2D} = Jk_x\left(k_x^2 - 3k_y^2\right)\sigma_z, \tag{4}$$

$$H_g^{2D} = Jk_xk_y\left(k_x^2 - k_y^2\right)\sigma_z, \tag{5}$$

$$H_i^{2D} = Jk_xk_y\left(3k_x^2 - k_y^2\right)\left(k_x^2 - 3k_y^2\right)\sigma_z. \tag{6}$$

Their tight-binding representation is constructed by replacing $k_j \mapsto \sin ak_j$, $k_j^2 \mapsto 2(1-\cos ak_j)$ with $j = x, y$ and the lattice constant a.

So far, we have discussed two-dimensional magnets. In a similar way, there are three-dimensional magnets with higher-wave symmetries [12,13] as summarized in Figs. 1(a2)–1(f2). The simplest expressions on magnetic terms with higher symmetries in three dimensions are summarized as follows:

$$H_d^{3D} = Jk_z(k_x + k_y)\sigma_z, \tag{7}$$

$$H_f^{3D} = Jk_xk_yk_z\sigma_z, \tag{8}$$

$$H_g^{3D} = Jk_zk_x\left(k_x^2 - 3k_y^2\right)\sigma_z, \tag{9}$$

$$H_i^{3D} = J\left(k_x^2 - k_y^2\right)\left(k_y^2 - k_z^2\right)\left(k_z^2 - k_x^2\right)\sigma_z. \tag{10}$$

Their tight-binding representation is constructed by replacing $k_j \mapsto \sin ak_j$, $k_j^2 \mapsto 2(1-\cos ak_j)$ with $j = x, y, z$.

III. NONLINEAR DRUDE CONDUCTIVITY

The Drude conductivity is the linear conductivity. It was generalized to the second-order nonlinear Drude conductivity [16,33]. The third-order nonlinear Drude conductivity was also derived [34]. They are derived in the static limit. We derive the ℓth order nonlinear Drude conductivity for a single band system for an arbitrary ℓ, which is valid even in the nonstatic regime. In the clean limit, the Drude conductivity is dominant.

The current is given by

$$\mathbf{j} = -e\int d^Dk f\mathbf{v}, \tag{11}$$

where D is the dimension; f is the Fermi distribution function in the presence of $\mathbf{E}$, and $\mathbf{v}$ is the velocity,

$$\mathbf{v} = \frac{1}{\hbar}\frac{\partial\varepsilon}{\partial\mathbf{k}}, \tag{12}$$

where ε is the energy of the Hamiltonian and we have dropped the anomalous velocity term proportional to $-e\mathbf{E}\times\mathbf{\Omega}/\hbar$ because the Berry curvature $\mathbf{\Omega}$ is zero due to the single band condition.

Let us present formulas in two dimensions. The generalization to three dimensions is straightforward. We expand the current in terms of electric field E as

$$j_b = \sum_{\ell_1,\ell_2=0} \sigma^{x^{\ell_1}y^{\ell_2};b}(E_x)^{\ell_1}(E_y)^{\ell_2}. \tag{13}$$

Then, the $(\ell_1+\ell_2)$th order conductivity is defined by

$$\sigma^{x^{\ell_1}y^{\ell_2};b} = \frac{1}{\ell_1!\ell_2!}\frac{\partial^{\ell_1+\ell_2}j_b}{\partial E_x^{\ell_1}\partial E_y^{\ell_2}}. \tag{14}$$

The semiclassical Boltzmann equation in the presence of electric field $\mathbf{E}$ is given by

$$\partial_t f - \frac{e\mathbf{E}}{\hbar}\cdot\nabla_{\mathbf{k}} f = -\frac{f-f^{(0)}}{\tau}, \tag{15}$$

where τ is the relaxation time and $f^{(0)}$ is the Fermi distribution function at the equilibrium with the chemical potential μ:

$$f^{(0)} = 1/(\exp[(\varepsilon-\mu)/k_BT]+1), \tag{16}$$

where k_B is the Boltzmann constant and T is the temperature. Corresponding to Eq. (13), we expand the Fermi distribution in powers of $\mathbf{E}$:

$$f = f^{(0)} + f^{(1)} + \cdots . \tag{17}$$

The recursive solution gives [34]

$$f^{(\ell_1+\ell_2)} = \left(\frac{e/\hbar}{i\omega + 1/\tau}\right)^{\ell_1+\ell_2} \frac{\partial^{\ell_1+\ell_2} f^{(0)}}{\partial k_x^{\ell_1} \partial k_y^{\ell_2}} (E_x)^{\ell_1} (E_x)^{\ell_2}, \tag{18}$$

where ω is the frequency of the applied electric field $\mathbf{E}$. The current (11) is expanded as in Eq. (17) with

$$\begin{aligned} j_b^{(\ell_1+\ell_2)} &= -e \int d^D k f^{(\ell_1+\ell_2)} v_b \\ &= -\frac{e}{\hbar}\left(\frac{e/\hbar}{i\omega + 1/\tau}\right)^{\ell_1+\ell_2} \\ &\quad \times \int d^D k \, \frac{\partial \varepsilon}{\partial k_b} \frac{\partial^{\ell_1+\ell_2} f^{(0)}}{\partial k_x^{\ell_1} \partial k_y^{\ell_2}} (E_x)^{\ell_1} (E_x)^{\ell_2}. \end{aligned} \tag{19}$$

The $(\ell_1 + \ell_2)$th nonlinear Drude conductivity is defined by

$$\sigma^{x^{\ell_1} y^{\ell_2}; b} = \frac{(-e/\hbar)^{\ell_1+\ell_2+1}}{(i\omega + 1/\tau)^{\ell_1+\ell_2}} \int d^D k f^{(0)} \frac{\partial^{\ell_1+\ell_2+1} \varepsilon}{\partial k_x^{\ell_1} \partial k_y^{\ell_2} \partial k_b}. \tag{20}$$

The static limit is obtained simply by setting $\omega = 0$ in this equation.

In this paper, we consider a Hamiltonian where the spin is a good quantum number, $\sigma_z = s = \pm 1$. We can define the ℓth order spin-dependent Drude conductivity for each spin s by the formula

$$\sigma_s^{x^{\ell_1} y^{\ell_2}; b} = \frac{(-e/\hbar)^{\ell_1+\ell_2+1}}{(i\omega + 1/\tau)^{\ell_1+\ell_2}} \int d^D k \, f_s^{(0)} \frac{\partial^{\ell_1+\ell_2+1} \varepsilon_s}{\partial k_x^{\ell_1} \partial k_y^{\ell_2} \partial k_b}, \tag{21}$$

where $s = \uparrow, \downarrow$. Let us use $s = \uparrow, \downarrow$ within indices and $s = \pm 1$ in equations. This formula is nontrivial only when

$$\frac{\partial^{\ell_1+\ell_2+1} \varepsilon_s}{\partial k_x^{\ell_1} \partial k_y^{\ell_2} \partial k_b} \neq 0, \tag{22}$$

which leads to a conclusion that there is no ℓth order nonlinear spin-Drude conductivity for $\ell \geqslant \ell_1 + \ell_2$. It is necessary to calculate explicitly the ℓth order nonlinear spin-Drude conductivity for $\ell = 0, 1, \ldots, \ell_1 + \ell_2 - 1$. In particular, the choice of $\ell = 0$ and 1 yield the persistent spin current without electric field and the linear spin conductivity, respectively.

We define the $(\ell_1 + \ell_2)$th order nonlinear spin-Drude conductivity by

$$\sigma_{\text{spin}}^{x^{\ell_1} y^{\ell_2}; b} = \frac{\sigma_\uparrow^{x^{\ell_1} y^{\ell_2}; b} - \sigma_\downarrow^{x^{\ell_1} y^{\ell_2}; b}}{2}. \tag{23}$$

On the other hand, the charge conductivity is given by

$$\sigma_{\text{charge}}^{x^{\ell_1} y^{\ell_2}; b} = \sigma_\uparrow^{x^{\ell_1} y^{\ell_2}; b} + \sigma_\downarrow^{x^{\ell_1} y^{\ell_2}; b}. \tag{24}$$

In the following sections, we calculate Eq. (21) for various higher-wave symmetric magnets.

In general, there are other contributions to the nonlinear conductivity from the quantum metric and the Berry curvature dipole for multiband system [14–28]. In the present model, the Hamiltonian is diagonal with respect to the spin degrees of freedom, and hence the system is an essentially single-band system. Hence, there is no contribution in the nonlinear conductivity from the quantum metric and the Berry curvature dipole.

The kinetic energy of free fermions is described by the Hamiltonian

$$H_0^{\text{2D}} = \frac{\hbar^2 (k_x^2 + k_y^2)}{2m} \sigma_0 \tag{25}$$

in two dimensions, and

$$H_0^{\text{3D}} = \frac{\hbar^2 (k_x^2 + k_y^2 + k_z^2)}{2m} \sigma_0 \tag{26}$$

in three dimensions, where m is the free-fermion mass and σ_0 is the 2×2 identity matrix.

The linear longitudinal charge conductivity is always present due to the kinetic Hamiltonian (25) or (26),

$$\sigma_{\text{charge}}^{x;x} = \frac{(e/\hbar)^2}{i\omega + 1/\tau} (V_\uparrow^{\text{F}} + V_\downarrow^{\text{F}}), \tag{27}$$

where V_s^{F} is the spin-dependent Fermi volume,

$$V_s^{\text{F}} \equiv \int d^D k f_s^{(0)}, \tag{28}$$

and we have used the relation (21), or

$$\sigma_s^{x;x} = \frac{(e/\hbar)^2}{i\omega + 1/\tau} \int d^D k \frac{\partial^2 \varepsilon}{\partial k_x^2} f_s^{(0)} = \frac{(e/\hbar)^2}{i\omega + 1/\tau} V_s^{\text{F}}. \tag{29}$$

On the other hand, the magnetic terms with higher symmetries generate transverse spin currents. We investigate linear and nonlinear transverse spin conductivities by taking the input and output along the x, y, and z axes.

IV. *s*-WAVE MAGNET IN 2D AND 3D

We consider the Hamiltonian of the s-wave magnet given by

$$H^{\text{total}} = H_0 + H_s, \tag{30}$$

where $H_0 = H_0^{\text{2D}}$ in two dimensions and $H_0 = H_0^{\text{3D}}$ in three dimensions with

$$H_s = J\sigma_z. \tag{31}$$

This system describes a ferromagnet.

The Fermi surface is determined by solving

$$\frac{\hbar^2 k^2}{2m} + sJ = \mu, \tag{32}$$

which is a circle with the radius k_s^{F} depending on the spin s:

$$\hbar k_s^{\text{F}} = \sqrt{2m(\mu - sJ)}. \tag{33}$$

The Fermi volume is

$$V_s^{\text{F}} = \frac{\pi}{\hbar^2}(2m\mu - sJ) \tag{34}$$

in two dimensions and

$$V_s^{\text{F}} = \frac{4\pi}{3\hbar^3}(2m\mu - sJ)^{3/2} \tag{35}$$

in three dimensions. They are shown in Figs. 1(a1) and 1(a2).

It follows from the condition (22) that there is no ℓth order spin-Drude conductivity for all $\ell \geqslant 2$. We examine explicitly

the spin conductivity for $\ell = 0, 1$ in the two-dimensional system. We examine all the nontrivial ones in the condition (22),

$$\frac{\partial \varepsilon_s}{\partial k_x} = \frac{\hbar^2 k_x}{m}, \quad \frac{\partial \varepsilon_s}{\partial k_y} = \frac{\hbar^2 k_y}{m},$$
$$\frac{\partial^2 \varepsilon_s}{\partial k_x^2} = \frac{\partial^2 \varepsilon_s}{\partial k_y^2} = \frac{\hbar^2}{m}, \tag{36}$$

which arise from the kinetic term (25).

We examine the spin current for $\ell = 0$, which corresponds to the persistent spin current without electric field. It is given by

$$j_x^{(0)} = -\frac{e}{\hbar}\int d^2k \frac{\partial \varepsilon}{\partial k_x} f_s^{(0)} = -\frac{e\hbar}{m}\int d^2k\, k_x f_s^{(0)} = 0, \tag{37}$$

because the integrand is an odd function of k_x.

We next examine the linear spin conductivity with $\ell = 1$. It is given by

$$\sigma_s^{x;x} = \frac{e}{\hbar}\int d^2k \frac{\partial^2 \varepsilon}{\partial k_x^2} f_s^{(0)} = \frac{e\hbar}{m} V_s^{\rm F}, \tag{38}$$

where $V_s^{\rm F}$ is the spin-dependent Fermi volume (34). Hence, we obtain

$$\sigma_{\rm spin}^{x;x} = \frac{\sigma_\uparrow^{x;x} - \sigma_\downarrow^{x;x}}{2} = \frac{e\hbar}{m}\frac{V_\uparrow^{\rm F} - V_\downarrow^{\rm F}}{2}, \tag{39}$$

implying that there follows a spin-polarized current in ferromagnet, where both charge and spin currents flow. The three-dimensional system is similarly analyzed with similar conclusion.

V. *p*-WAVE MAGNET IN 2D

We consider the Hamiltonian of the p-wave magnet in two dimensions given by

$$H^{\rm total} = H_0^{\rm 2D} + H_p. \tag{40}$$

The second term represents the p-wave magnet [10,35–39],

$$H_p = J\sigma_z k_x. \tag{41}$$

The spin-dependent Hamiltonian is explicitly written as

$$H_s^{\rm total} = \frac{\hbar^2\left(k_x^2 + k_y^2\right)}{2m} + sJk_x$$
$$= \frac{\hbar^2}{2m}\left(k_x + \frac{msJ}{\hbar^2}\right)^2 + \frac{\hbar^2 k_y^2}{2m} - \frac{mJ^2}{2\hbar^2}. \tag{42}$$

The Fermi surface is a circle for each spin s as shown in Fig. 1(b1).

We make a change of variable from k_x to k_x':

$$k_x' \equiv k_x + \frac{msJ}{\hbar^2}. \tag{43}$$

The Hamiltonian is rewritten as

$$H_s^{\rm total} = \frac{\hbar^2\left(k_x'^2 + k_y^2\right)}{2m} - \frac{mJ^2}{2\hbar^2}, \tag{44}$$

which has the form of the free fermion. The Fermi surface is described by

$$\hbar k'^{\rm F} = \sqrt{2m\left(\mu + \frac{mJ^2}{2\hbar^2}\right)} \tag{45}$$

and the Fermi volume is

$$V^{\rm F} = \frac{2\pi m}{\hbar^2}\left(\mu + \frac{mJ^2}{2\hbar^2}\right). \tag{46}$$

Because both the Hamiltonian and the Fermi surfaces are independent of the spin s in the (k_x', k_y) space, there is no ℓth order spin-Drude conductivity (23) for all $\ell \geqslant 0$.

A comment is in order. The Fermi surfaces of the p-wave magnet are peculiar in comparison with all others in Fig. 1, where the Fermi surfaces are shifted oppositely for the opposite spins, as shown in Fig. 1(b2). Hence, one might assume that there must be a net spin current with $\ell = 0$, $\sigma_{\rm spin}^{;x} \neq 0$, implying the existence of a persistent spin current without electric field. This intuitive picture would be correct if fermions were free fermions, where

$$v_x = \hbar k_x/m. \tag{47}$$

Then, because $f_s^{(0)} k_x'$ is an odd function of k_x', the current would be

$$j_x^{(0)} = -e\int d^2k f_s^{(0)} v_x = -\frac{e\hbar}{m}\int d^2k' f_s^{(0)}\left(k_x' - \frac{sJ}{\hbar^2}\right)$$
$$= sJ\frac{e}{m\hbar}V^{\rm F}, \tag{48}$$

where $V^{\rm F}$ is the Fermi volume. It would imply the existence of the persistent spin current without external electric field E. However, this is not correct because fermions are not free fermions. The velocity is determined by the formula (12),

$$v_x = \hbar k_x/m + sJ/\hbar, \tag{49}$$

and not by Eq. (47). These two terms cancel each other to produce no persistent spin current without external field E.

For the sake of completeness, let us calculate explicitly the persistent spin-dependent current without external field E. The current is given by Eq. (11) with the choice of $\ell = 0$, which is calculated as

$$j_x^{(0)} = -e\int d^2k f_s^{(0)} v_x = -\frac{e}{\hbar}\int d^2k' \frac{\partial k_x'}{\partial k_x}\frac{\partial \varepsilon_s}{\partial k_x'} f_s^{(0)}$$
$$= -\frac{e}{\hbar}\int d^2k' \frac{\partial \varepsilon_s}{\partial k_x'} f_s^{(0)} = -\frac{e\hbar}{m}\int d^2k'\, k_x' f_s^{(0)} = 0. \tag{50}$$

Hence, no zeroth spin current is generated, i.e., $\sigma_{\rm spin}^{;x} = 0$.

Next, we calculate the linear spin-dependent conductivity ($\ell = 1$). In the (k_x', k_y) space, we obtain

$$\sigma_s^{x;x} = \frac{e^2/\hbar^2}{i\omega + 1/\tau}\int d^2k' \frac{\partial^2 \varepsilon_s}{\partial k_x'^2} f^{(0)}$$
$$= \frac{e^2/m}{i\omega + 1/\tau}\int d^2k' f^{(0)} = \frac{e^2/m}{i\omega + 1/\tau}V^{\rm F}. \tag{51}$$

This is independent of the spin s, and hence, $\sigma^{x;x}_{\rm spin}=0$. However, the linear charge conductivity is generated:

$$\sigma^{x;x}_{\rm charge}\equiv\sigma^{x;x}_{\uparrow}+\sigma^{x;x}_{\downarrow}=\frac{4e\pi}{\hbar}\left(\mu+\frac{mJ^2}{2\hbar^2}\right). \tag{52}$$

It is interesting that the linear charge conductivity has a J dependence.

The tight-binding model corresponding to the continuum model (40) is given by

$$H^{\rm 2D}_0=\frac{\hbar^2}{ma^2}(2-\cos ak_x-\cos ak_y)\sigma_0+J\sigma_z\sin ak_x, \tag{53}$$

which is defined on the square lattice.

VI. *p*-WAVE MAGNET IN 3D

We consider the Hamiltonian of a p-wave magnet in three dimensions given by

$$H^{\rm total}=H^{\rm 3D}_0+H_p. \tag{54}$$

The second term represents the p-wave magnet:

$$H_p=J\sigma_z k_x. \tag{55}$$

The Fermi surface is shown in Fig. 1(b2).

Making a change of variable from k_x to k'_x as in Eq. (43), the Hamiltonian is rewritten as

$$H_s=\frac{\hbar^2\left(k_x'^2+k_y^2+k_z^2\right)}{2m}-\frac{mJ^2}{2\hbar^2}, \tag{56}$$

which has the form of the free fermion. The Fermi surface is described by

$$\hbar k'^{\rm F}=\sqrt{2m\left(\mu+\frac{mJ^2}{2\hbar^2}\right)}. \tag{57}$$

There is no ℓth order spin-Drude conductivity for all $\ell\geqslant 0$ as in the two-dimensional system. The physics is essentially identical to the p-wave magnet in two dimensions.

The tight-binding model corresponding to the continuum model (54) is given by

$$H^{\rm 2D}_0=\frac{\hbar^2}{ma^2}(3-\cos ak_x-\cos ak_y-\cos ak_z)\sigma_0+J\sin ak_x\sigma_z, \tag{58}$$

which is defined on the cubic lattice.

VII. *d*-WAVE ALTERMAGNET IN 2D

We analyze the Hamiltonian

$$H^{\rm total}=H^{\rm 2D}_0+H^{\rm 2D}_d. \tag{59}$$

The second term represents the d-wave altermagnet [12,13,40–45],

$$H^{\rm 2D}_d=Jk_xk_y\sigma_z. \tag{60}$$

The spin-dependent energy is explicitly written as

$$\varepsilon_s=\frac{\hbar^2\left(k_x^2+k_y^2\right)}{2m}+sJk_xk_y. \tag{61}$$

We examine the condition (22). We list all the nontrivial ones,

$$\frac{\partial\varepsilon_s}{\partial k_x}=\frac{\hbar^2k_x}{m}+sJk_y,\quad \frac{\partial\varepsilon_s}{\partial k_y}=\frac{\hbar^2k_y}{m}+sJk_x,$$
$$\frac{\partial^2\varepsilon_s}{\partial k_x^2}=\frac{\partial^2\varepsilon_s}{\partial k_y^2}=\frac{\hbar^2}{m},\quad \frac{\partial^2\varepsilon_s}{\partial k_y\partial k_x}=sJ, \tag{62}$$

with ε_s given by Eq. (61), which could contribute only to the spin conductivity for $\ell=0,1$. There is no ℓth order nonlinear spin-Drude conductivity for all $\ell\geqslant 2$. It is straightforward to see that there is no spin conductivity for $\ell=0$.

We study the linear spin conductivity $\sigma^{y;x}_{\rm spin}$ and $\sigma^{x;x}_{\rm spin}$ corresponding to the choice of $\ell=1$. Note that $\sigma^{y;x}_{\rm spin}=\sigma^{x;y}_{\rm spin}$ and $\sigma^{x;x}_{\rm spin}=\sigma^{y;y}_{\rm spin}$ due to the symmetry of the Hamiltonian under the exchange of k_x and k_y. We introduce the polar coordinate $k_x=k\cos\phi$ and $k_y=k\sin\phi$. The Fermi surface is analytically obtained as a function of ϕ:

$$\hbar k^{\rm F}_s(\phi)=\sqrt{\frac{2\mu}{\frac{1}{m}+sJ\sin 2\phi}}. \tag{63}$$

It is shown for each spin s in Fig. 1(c1). The Fermi volume is given by

$$V^{\rm F}\equiv\int d^2k f^{(0)}_s=\frac{2\pi m\mu}{\hbar^2\sqrt{1-J^2m^2}}, \tag{64}$$

which is obtained with the use of (63) for $|Jm|<1$. This is the condition that the energy (61) is positive for sufficiently large momentum. The J dependence of the Fermi volume $V^{\rm F}$ is shown in Fig. 3(a).

First, we calculate the linear longitudinal spin-dependent conductivity $\sigma^{x;x}_s$. We obtain

$$\sigma^{x;x}_s=\frac{e^2/\hbar^2}{i\omega+1/\tau}\frac{\hbar^2}{m}V^{\rm F}, \tag{65}$$

which yields $\sigma^{x;x}_{\rm spin}=0$, because $\sigma^{x;x}_s$ is independent of the spin s.

Next, we calculate the linear transverse spin-dependent conductivity $\sigma^{y;x}_s$:

$$\sigma^{y;x}_s=\sigma^{x;y}_s=s\frac{e^2/\hbar^2}{i\omega+1/\tau}V^{\rm F}J. \tag{66}$$

Hence, this spin conductivity is obtained as

$$\sigma^{y;x}_{\rm spin}=\sigma^{x;y}_{\rm spin}=\frac{e^2/\hbar^2}{i\omega+1/\tau}V^{\rm F}J, \tag{67}$$

with the use of the Fermi volume (64). The J dependence of the $\sigma^{y;x}_{\rm spin}$ is shown in Fig. 4(a). We conclude that there is only linear spin conductivity.

The tight-binding model corresponding to the continuum model (59) is given by

$$H=\frac{1}{m}(2-\cos k_x-\cos k_y)\sigma_0+J\sigma_z\sin k_x\sin k_y, \tag{68}$$

which is defined on the square lattice.

We calculate the spin-Drude conductivity $\sigma^{y;x}_{\rm spin}$ based on the continuum model and the tight-binding model, which are shown in Fig. 2(a). They agree with each other very well in

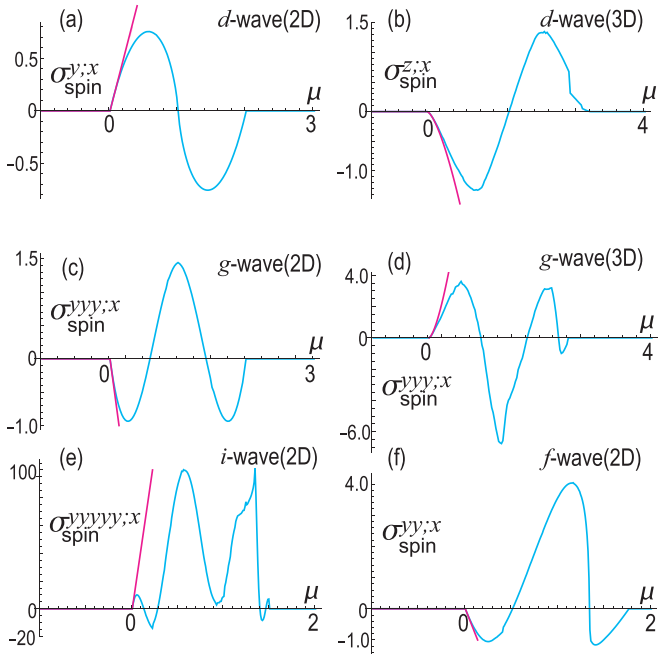

FIG. 2. μ dependence of the spin-Drude conductivity in units of $e^\ell \tau^{\ell-1}\varepsilon_0/(\hbar^\ell k_0)$. (a) The d-wave magnet ($\ell = 1$) in 2D, (b) the d-wave magnet ($\ell = 1$) in 3D, (c) the g-wave magnet ($\ell = 3$) in 2D, (d) the g-wave magnet ($\ell = 3$) in 3D, (e) the i-wave magnet ($\ell = 5$) in 2D, (f) the f-wave magnet ($\ell = 2$) in 2D. Cyan curves represent numerical results based on tight-binding models, while magenta curves represent analytical results based on continuum models. The horizontal axis is μ in units of ε_0.We have set $\hbar^2/(ma^2) = \varepsilon_0/4$ and $J = 0.1\varepsilon_0$.

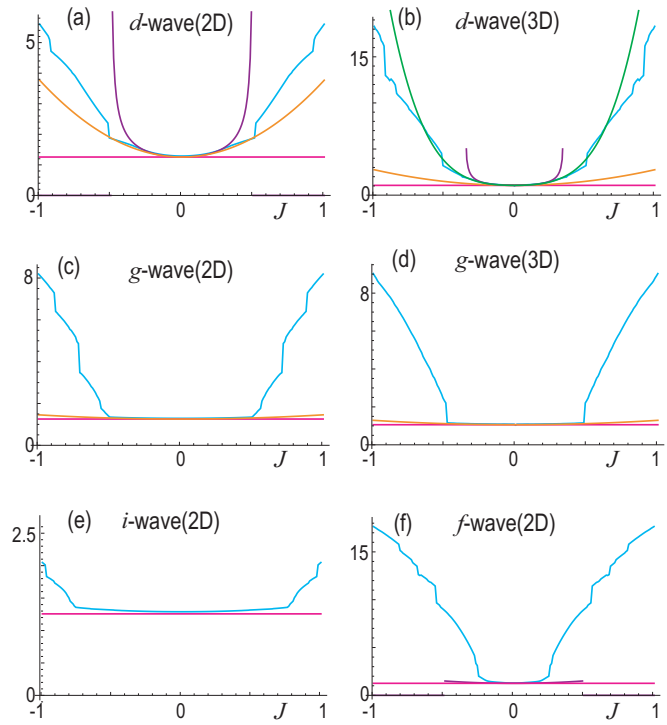

FIG. 3. J dependence of the Fermi volume $V^{\rm F}$. (a) d-wave magnet in 2D. (b) d-wave magnet in 3D. (c) g-wave magnet in 2D. (d) g-wave magnet in 3D. (e) i-wave magnet in 2D. (f) f-wave magnet in 2D. Cyan curves represent numerical results based on tight-binding models. Purple curves represent analytical results based on continuum models. Magenta (orange, green) lines represent analytical results up to the zeroth (second, fourth) order in J. The vertical axis is the Fermi volume in units of $2\pi m\mu/\hbar^2$ in two dimensions and $8\sqrt{2}\pi(m\mu)^{3/2}/(3\hbar^3)$ in three dimensions. The horizontal axis is J in units of ε_0. We have set $\hbar^2/(ma^2) = \varepsilon_0/4$ and $\mu = 0.1\varepsilon_0$.

the vicinity of the band bottom $\mu = 0$. The analytical result of the Fermi volume (64) coincides well with the tight-binding result for small J as shown in Fig. 3(a). The result (67) is only valid for $|Jm| < 1$ as shown in the purple curve in Fig. 3(a). However, by making a series expansion up to the second order in J, the fitting becomes better as shown in the orange curve in Fig. 3(a). The J dependence of the $\sigma^{y;x}_{\rm spin}$ is shown in Fig. 4(a), which is obtained numerically based on the tight-binding model. The numerical and analytic results agree well for $|Jm| < 1$.

VIII. d-WAVE ALTERMAGNET IN 3D

We consider the Hamiltonian of the d-wave altermagnet in three dimensions given by

$$H^{\rm total} = H_0^{\rm 3D} + H_d^{\rm 3D}. \tag{69}$$

The second term represents the d-wave altermagnet [12]:

$$H_d^{\rm 3D} = Jk_z(k_x + k_y)\sigma_z. \tag{70}$$

The Fermi surface is analytically described in the spherical coordinate $k_x = k\cos\phi\sin\theta$, $k_y = k\sin\phi\sin\theta$ and $k_z = k\cos\theta$ as

$$\hbar k_s^{\rm F}(\phi,\theta) = \sqrt{\frac{2\mu}{\frac{1}{m} + sJ(\cos\phi + \sin\phi)\sin 2\theta}}, \tag{71}$$

which is shown in Fig. 1(c2). The Fermi volume is analytically obtained as

$$V^{\rm F} = \frac{8\sqrt{2}\pi(m\mu)^{3/2}}{3\hbar^3\sqrt{1-2J^2m^2}}. \tag{72}$$

It follows from the condition (22) that there is no ℓth order spin-Drude conductivity for all $\ell \geqslant 3$. It is straightforward to see that there is no spin conductivity for $\ell = 0$.

We calculate the linear longitudinal spin-dependent conductivity $\sigma_s^{x;x}$. Because

$$\frac{\partial^2\varepsilon}{\partial k_x^2} = \frac{\partial^2\varepsilon}{\partial k_y^2} = \frac{\partial^2\varepsilon}{\partial k_z^2} = \frac{\hbar^2}{m}, \tag{73}$$

we obtain

$$\sigma_s^{x;x} = \frac{e^2/m}{i\omega + 1/\tau}V^{\rm F} \tag{74}$$

with (72). This yields $\sigma^{x;x}_{\rm spin} = 0$, because $\sigma_s^{x;x}$ is independent of the spin s.

We next calculate the linear transverse spin-dependent conductivity $\sigma_s^{z;x}$. Because

$$\frac{\partial^2\varepsilon_s}{\partial k_z\partial k_x} = \frac{\partial^2\varepsilon_s}{\partial k_y\partial k_z} = sJ, \tag{75}$$

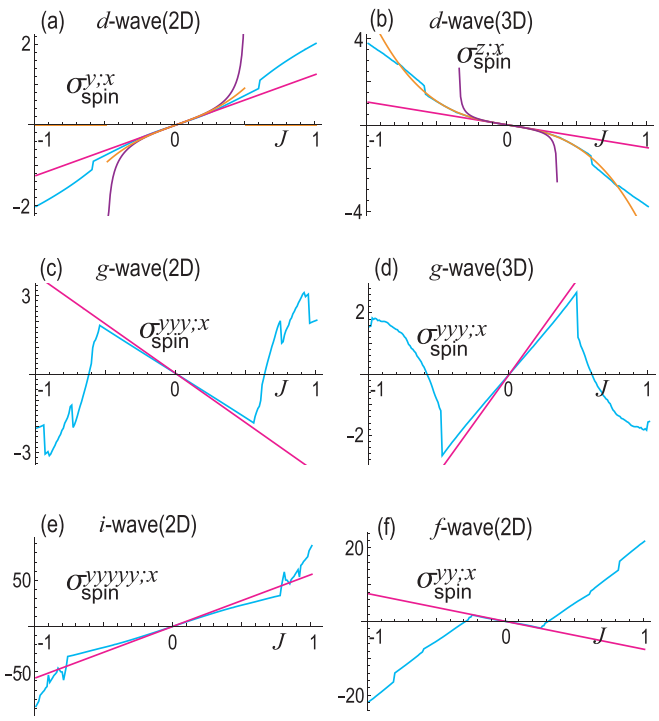

FIG. 4. J dependence of the spin-Drude conductivity. Cyan curves represent numerical results based on tight-binding models. Purple curves represent analytical results based on continuum models. Magenta (orange) lines represent analytical results up to the zeroth (second) order in J. The horizontal axis is J in units of ε_0. We have set $\hbar^2/(ma^2) = \varepsilon_0/4$ and $\mu = 0.1\varepsilon_0$. See the caption of Fig. 2 regarding others.

we obtain

$$\sigma_s^{z;x} = \sigma_s^{x;z} = \sigma_s^{z;y} = \sigma_s^{y;z} = s\frac{e^2/\hbar^2}{i\omega + 1/\tau}V^{\rm F}J. \tag{76}$$

Hence, the spin conductivity is obtained as

$$\sigma^{z;x}_{\rm spin} = \sigma^{x;z}_{\rm spin} = \sigma^{z;y}_{\rm spin} = \sigma^{y;z}_{\rm spin} = \frac{e^2/\hbar^2}{i\omega + 1/\tau}V^{\rm F}J, \tag{77}$$

The J dependence of the $\sigma^{z;x}_{\rm spin}$ is shown in Fig. 4(b). We conclude that there is only linear spin conductivity.

The tight-binding model corresponding to the continuum model (69) is given by

$$H = \frac{\hbar^2}{ma^2}(3 - \cos ak_x - \cos ak_y - \cos ak_z)\sigma_0 + J\sigma_z \sin ak_z(\sin ak_x + \sin ak_y), \tag{78}$$

which is defined on the cubic lattice. We calculate the spin-Drude conductivity based on the continuum model and the tight-binding model, which are shown in Fig. 2(b). They agree with each other very well in the vicinity of the band bottom $\mu = 0$. The Fermi surface is shown in Fig. 1(c2).

The J dependence of the Fermi volume V_s is shown in Fig. 3(b). The result (67) is only valid for $|Jm| < 1/\sqrt{2}$ as shown in the purple curve in Fig. 3(b). However, by making a series expansion up to the fourth order in J, the fitting becomes better as shown in the green curve in Fig. 3(b).

The J dependence of the $\sigma^{z;x}_{\rm spin}$ is shown in Fig. 4(b). The series expansion up to the second order in J well fits the result based on the tight-binding model as shown in the orange curve in Fig. 4(b).

IX. f-WAVE MAGNET IN 2D

A possibility of f-wave magnets has been mentioned [10,11]. The simplest Hamiltonian of the f-wave magnet in two dimensions is given by

$$H^{\rm total} = H_0^{\rm 2D} + H_f^{\rm 2D}. \tag{79}$$

The second term represents the f-wave magnet:

$$H_f = Jk_x\left(k_x^2 - 3k_y^2\right)\sigma_z. \tag{80}$$

The Fermi surface is described by

$$\hbar k_s^{\rm F}(\phi) = \sqrt{2\mu m} - 2m^2\mu sJ\cos 3\phi \tag{81}$$

up to the first order in J. The Fermi surfaces $k_s^{\rm F}(\phi)$ for up and down spins are shown in Fig. 1(d1). Then, the Fermi volume is analytically obtained as

$$V^{\rm F} = \frac{2\pi m\mu}{\hbar^2}(1 + \mu m^3J^2), \tag{82}$$

up to the second order in J. It is independent of spin s.

We list all the nontrivial ones in the condition (22):

$$\frac{\partial\varepsilon_s}{\partial k_x} = \frac{\hbar^2}{m}k_x + 3sJ\left(k_x^2 - k_y^2\right),$$
$$\frac{\partial\varepsilon_s}{\partial k_y} = \frac{\hbar^2}{m}k_y - 6sJk_xk_y$$
$$\frac{\partial^2\varepsilon_s}{\partial k_x^2} = \frac{\hbar^2}{m} + 6sJk_x, \quad \frac{\partial^2\varepsilon_s}{\partial k_y^2} = \frac{\hbar^2}{m} - 6sJk_x,$$
$$\frac{\partial^2\varepsilon_s}{\partial k_x\partial k_y} = -6sJk_y,$$
$$\frac{\partial^3\varepsilon_s}{\partial k_x\partial k_y^2} = -6sJ, \quad \frac{\partial^3\varepsilon_s}{\partial k_x^3} = 6sJ. \tag{83}$$

They could produce the spin conductivity (21) only for $\ell = 0, 1, 2$. There is no ℓth-order nonlinear spin-Drude conductivity for $\ell \geqslant 3$.

We examine the spin conductivity for $\ell = 0, 1, 2$. Calculating them explicitly, we find that the nontrivial results are given only by the terms $\partial^3\varepsilon_s/\partial k_x\partial k_y^2$ and $\partial^3\varepsilon_s/\partial k_x^3$, yielding

$$\int d^2k f_s^{(0)}\frac{\partial^3\varepsilon_s}{\partial k_y^2\partial k_x} = -\int d^2k f_s^{(0)}\frac{\partial^3\varepsilon_s}{\partial k_x^3} = -6sV^{\rm F}J, \tag{84}$$

where $V^{\rm F}$ is the Fermi volume (82). The second-order nonlinear spin-Drude conductivity is given by

$$\sigma^{yy;x}_{\rm spin} = \sigma^{xy;y}_{\rm spin} = 6\frac{(e/\hbar)^3}{(i\omega + 1/\tau)^2}V^{\rm F}J,$$
$$\sigma^{xx;x}_{\rm spin} = -6\frac{(e/\hbar)^3}{(i\omega + 1/\tau)^2}V^{\rm F}J. \tag{85}$$

We conclude that there is only the second-order nonlinear spin-Drude conductivity.

The tight-binding model corresponding to the continuum model (79) is given by

$$H = \frac{-2\hbar^2}{3ma^2}\left(\sum_{j=1}^{3}\cos(a\mathbf{n}_j\cdot\mathbf{k})-3\right)\sigma_0 - 4J\sigma_z\prod_{j=1}^{3}\sin(a\mathbf{n}_j\cdot\mathbf{k}). \tag{86}$$

We calculate the spin-Drude conductivity based on the continuum model and the tight-binding model, which are shown in Fig. 2(f). They agree each other very well in the vicinity of the band bottom $\mu = 0$.

The second-order nonlinear conductivity shows a nonreciprocity because the current flowing direction is identical irrespective of the direction of applied electric field. Especially, the nonreciprocity is perfect because there is only second-order nonlinear conductivity in the f-wave magnet.

The J dependence of the $\sigma^{yy;x}$ is shown in Fig. 4(f). The $\sigma^{yy;x}$ is linear in J in a wide range of J. The J dependence of the Fermi volume $V^{\rm F}$ is shown in Fig. 3(f). There is almost no J dependence in the Fermi volume for small J.

X. f-WAVE MAGNET IN 3D

We consider the Hamiltonian of the f-wave magnet in three dimensions given by

$$H^{\rm total} = H_0^{\rm 3D} + H_f^{\rm 3D}. \tag{87}$$

The second term represents the f-wave magnet:

$$H_f^{\rm 3D} = Jk_xk_yk_z\sigma_z. \tag{88}$$

The Fermi surface is described by

$$\hbar k_s^{\rm F}(\phi,\theta) = \sqrt{2\mu m} - \mu m^2 sJ\cos\theta\sin^2\theta\sin 2\phi \tag{89}$$

up to the first order in J, which is a constant and independent of the spin s. The Fermi volume is given by

$$V^{\rm F} = \frac{8\sqrt{2}\pi(m\mu)^{3/2}}{3\hbar^3} + \frac{16\sqrt{2}}{105\hbar^3}\mu^2J^2m^4\sqrt{m}\pi \tag{90}$$

up to the second order in J.

There is no ℓth order spin-Drude conductivity for all $\ell \geqslant 3$. It is straightforward to see that there is no spin conductivity for $\ell = 0, 1$. We calculate the nonlinear spin-dependent conductivity with $\ell = 2$. Because

$$\frac{\partial^3\varepsilon_s}{\partial k_x\partial k_y\partial k_z} = sJ, \tag{91}$$

we obtain the nonlinear spin-Drude conductivity:

$$\sigma_{\rm spin}^{zy;x} = -\frac{(e/\hbar)^3}{(i\omega+1/\tau)^2}V^{\rm F}J. \tag{92}$$

We conclude that there is only second-order nonlinear spin-Drude conductivity.

The tight-binding model corresponding to the continuum model (87) is given by

$$H = \frac{\hbar^2}{ma^2}(3-\cos ak_x-\cos ak_y-\cos ak_z)\sigma_0 + J\sigma_z\sin ak_x\sin ak_y\sin ak_z, \tag{93}$$

which is defined on the cubic lattice. The Fermi surface is shown in Fig. 1(d2).

XI. g-WAVE ALTERMAGNET IN 2D

We consider the Hamiltonian of the g-wave altermagnet in two dimensions given by

$$H^{\rm total} = H_0^{\rm 2D} + H_g^{\rm 2D}. \tag{94}$$

The second term represents the g-wave altermagnet [12]:

$$H_g^{\rm 2D} = Jk_xk_y\left(k_x^2-k_y^2\right)\sigma_z. \tag{95}$$

The spin-dependent energy reads

$$\varepsilon_s = \frac{\hbar^2\left(k_x^2+k_y^2\right)}{2m} + sJk_xk_y\left(k_x^2-k_y^2\right). \tag{96}$$

The Fermi surface is described by

$$\hbar k_s^{\rm F}(\phi) = \sqrt{\frac{-1+\sqrt{1+4\mu sJm^2\sin 4\phi}}{sJm\sin 4\phi}}, \tag{97}$$

which is shown in Fig. 1(e1). The Fermi volume is obtained as

$$V^{\rm F} = \frac{2\pi m\mu}{\hbar^2}(1+\mu^2m^4J^2) \tag{98}$$

up to the second order in J.

There is no ℓth order nonlinear spin-Drude conductivity for all $\ell \geqslant 4$. We then explicitly calculate the spin current for $\ell = 0, 1, 2, 3$. The nontrivial conductivity arises only from the following terms:

$$\frac{\partial^4\varepsilon_s}{\partial k_y^3\partial k_x} = -6sJ, \quad \frac{\partial^4\varepsilon_s}{\partial k_x^3\partial k_y} = 6sJ. \tag{99}$$

They lead to the third-order nonlinear spin-Drude conductivity:

$$\sigma_{\rm spin}^{yyy;x} = \sigma_{\rm spin}^{xyy;y} = -6\frac{(e/\hbar)^4}{(i\omega+1/\tau)^3}V^{\rm F}J,$$
$$\sigma_{\rm spin}^{xxx;y} = \sigma_{\rm spin}^{xxy;x} = 6\frac{(e/\hbar)^4}{(i\omega+1/\tau)^3}V^{\rm F}J. \tag{100}$$

We conclude that there is only third-order nonlinear spin-Drude conductivity.

The tight-binding model corresponding to the continuum model (94) is given by

$$H_0^{\rm 2D} = \frac{\hbar^2}{ma^2}(2-\cos ak_x-\cos ak_y)\sigma_0 + J\sin ak_x\sin ak_y(\cos ak_x-\cos ak_y)\sigma_z, \tag{101}$$

which is defined on the square lattice. We calculate the spin-Drude conductivity based on the continuum model and the tight-binding model, which are shown in Fig. 2(c). They agree with each other very well in the vicinity of the band bottom $\mu = 0$.

The J dependence of the Fermi volume $V^{\rm F}$ is shown in Fig. 3(c). There is almost no J dependence in the Fermi volume for small J. The J dependence of the $\sigma_{\rm spin}^{yyy;x}$ is shown in Fig. 4(c). The $\sigma_{\rm spin}^{yyy;x}$ is linear in J in a wide range of J. It

means that the analytic result Eq. (100) is applicable to a wide range of J.

XII. g-WAVE ALTERMAGNET IN 3D

We consider the Hamiltonian of the g-wave altermagnet in three dimensions given by

$$H^{\text{total}} = H_0^{\text{3D}} + H_g^{\text{3D}}. \tag{102}$$

The second term represents the g-wave altermagnet in three dimensions [12]:

$$H_g^{\text{3D}} = Jk_zk_x\left(k_x^2 - 3k_y^2\right)\sigma_z. \tag{103}$$

The Fermi surface is described by

$$\hbar k_s^{\text{F}}(\phi,\theta) = \sqrt{\frac{-1+\sqrt{1+16\mu sJm^2\cos\theta\cos 3\phi\sin^3\theta}}{sJm\sin^3\theta\cos\theta\cos 3\phi}}, \tag{104}$$

which is shown as s in Fig. 1(e1). The Fermi volume is obtained as

$$V^{\text{F}} = \frac{8\sqrt{2}\pi(m\mu)^{3/2}}{3\hbar^3} + \frac{128\sqrt{2}\pi m^{11/2}\mu^{7/2}J^2}{35\hbar^3} \tag{105}$$

up to the second order in J. It is independent of the spin s.

There is no ℓth-order spin-Drude conductivity for all $\ell \geqslant 4$. It is straightforward to see that there is no spin conductivity for $\ell = 0, 1, 2$.

We calculate the nonlinear spin-dependent conductivity with $\ell = 3$. Because

$$\frac{\partial^4\varepsilon_s}{\partial k_x^3\partial k_z} = -\frac{\partial^4\varepsilon_s}{\partial k_x\partial k_y^2\partial k_z} = 6sJ, \tag{106}$$

we obtain

$$\sigma_{\text{spin}}^{xxx;z} = 6\frac{(e/\hbar)^4}{(i\omega+1/\tau)^3}V^{\text{F}}J. \tag{107}$$

We conclude that there is only third-order nonlinear spin-Drude conductivity.

The tight-binding model corresponding to the continuum model (102) is given by

$$H = \left[\frac{-2\hbar^2}{3ma^2}\left(\sum_{j=1}^{3}\cos a\mathbf{n}_j\cdot\mathbf{k} - 3\right) + \frac{\hbar^2}{m_za^2}(1-\cos ak_z)\right]\sigma_0 - 4J\sigma_z\sin ak_z\prod_{j=1}^{3}\sin a\mathbf{n}_j\cdot\mathbf{k}, \tag{108}$$

where we have defined

$$\mathbf{n}_j = \left(\cos\frac{2\pi j}{3}, \sin\frac{2\pi j}{3}\right), \tag{109}$$

with $j = 0, 1, 2$ and $\mathbf{k} = (k_x, k_y)$. It is defined on the layered triangular lattice. The Fermi surface is shown in Fig. 1(e2).

We calculate the spin-Drude conductivity based on the continuum model and the tight-binding model, which are shown in Fig. 2(d). They agree very well in the vicinity of the band bottom $\mu = 0$.

The J dependence of the Fermi volume V_s^{F} is shown in Fig. 3(d). There is almost no J dependence in the Fermi volume for small J. The J dependence of the $\sigma_{\text{spin}}^{xxx;z}$ is shown in Fig. 4(d). The $\sigma_{\text{spin}}^{xxx;z}$ is linear in J in a wide range of J. It means that the analytic result Eq. (107) is applicable to a wide range of J.

XIII. i-WAVE ALTERMAGNET IN 2D

We consider the Hamiltonian of the i-wave altermagnet in two dimensions given by

$$H^{\text{total}} = H_0^{\text{2D}} + H_i^{\text{2D}}. \tag{110}$$

The second term represents the i-wave altermagnet [12]:

$$H_i^{\text{2D}} = Jk_xk_y\left(3k_x^2 - k_y^2\right)\left(k_x^2 - 3k_y^2\right)\sigma_z. \tag{111}$$

The Fermi surfaces for up and down spins are shown in Fig. 1(f1).

The Fermi surface is described by

$$\hbar k_s^{\text{F}}(\phi) = \sqrt{2m\mu}(1 - 2\mu^2m^3sJ\sin 6\phi) \tag{112}$$

up to the first order in J. The Fermi volume is analytically obtained as

$$V^{\text{F}} = \frac{2\pi m\mu}{\hbar^2}\left(1 + \frac{\mu^4m^6J^2}{2}\right) \tag{113}$$

up to the second order in J. It is independent of the spin s.

There is no ℓth order spin-Drude conductivity for all $\ell \geqslant 6$. It is straightforward to see that there is no spin conductivity for $\ell = 0, 1, 2, 3, 4$. We calculate the nonlinear spin-dependent conductivity for $\ell = 5$. The nontrivial conductivity arises only from the following terms:

$$\frac{\partial^6\varepsilon_s}{\partial k_y^5\partial k_x} = -\frac{\partial^6\varepsilon_s}{\partial k_y^3\partial k_x^3} = \frac{\partial^6\varepsilon_s}{\partial k_y\partial k_x^5} = 360sJ \tag{114}$$

and those obtained by changing x and y. The nontrivial spin-Drude conductivity is given by

$$\sigma_{\text{spin}}^{yyyyy;x} = \sigma_{\text{spin}}^{xxxxx;y} = -\sigma_{\text{spin}}^{xxxyy;y} = 360\frac{(e/\hbar)^6}{(i\omega+1/\tau)^5}V^{\text{F}}J. \tag{115}$$

We conclude that there is only fifth-order nonlinear spin-Drude conductivity.

The tight-binding model corresponding to the continuum model (110) is given by

$$H = \left[\frac{-2\hbar^2}{3ma^2}\left(\sum_{j=0}^{2}\cos\left(a\mathbf{n}_j^{\text{A}}\cdot\mathbf{k}\right) - 3\right) + \frac{\hbar^2}{m_za^2}(1-\cos ak_z)\right]\sigma_0 + 16J\sigma_z\sin ak_z\prod_{j=0}^{2}\sin\left(a\mathbf{n}_j^{\text{A}}\cdot\mathbf{k}\right)\prod_{j=0}^{2}\sin\left(\sqrt{3}a\mathbf{n}_j^{\text{B}}\cdot\mathbf{k}\right), \tag{116}$$

where we have defined

$$\mathbf{n}_j^{\text{A}} = \left(\cos\frac{2\pi j}{3}, \sin\frac{2\pi j}{3}\right), \quad \mathbf{n}_j^{\text{B}} = \left(\sin\frac{2\pi j}{3}, \cos\frac{2\pi j}{3}\right), \tag{117}$$

with $j = 0, 1, 2$. We calculate the spin-Drude conductivity based on the continuum model and the tight-binding model, which are shown in Fig. 2(e). They agree with each other very well in the vicinity of the band bottom $\mu = 0$.

The J dependence of the Fermi volume $V_s^{\rm F}$ is shown in Fig. 3(e). The J dependence of the $\sigma_{\rm spin}^{yyyyy;z}$ is shown in Fig. 4(e). The $\sigma_{\rm spin}^{yyyyy;z}$ is linear in J in a wide range of J. It means that the analytic result Eq. (115). is applicable to a wide range of J.

XIV. i-WAVE ALTERMAGNET IN 3D

We consider the Hamiltonian of a i-wave altermagnet in three dimensions given by

$$H^{\rm total} = H_0^{\rm 3D} + H_i^{\rm 3D}. \tag{118}$$

The first term represents the kinetic energy of free fermions [12]:

$$H_i^{\rm 3D} = J\left(k_x^2 - k_y^2\right)\left(k_y^2 - k_z^2\right)\left(k_z^2 - k_x^2\right)\sigma_z. \tag{119}$$

The Fermi surface is described by

$$\hbar k_s^{\rm F}(\phi,\theta) = \sqrt{2m\mu} - \sqrt{2m\mu}8\mu^2 m^3 sJ \sin^2\theta\cos 2\phi \times \left(\cos^2\theta - \sin^2\theta\cos^2\phi\right)\left(\sin^2\theta\sin^2\phi - \cos^2\theta\right) \tag{120}$$

up to the first order in J. The Fermi volume is analytically obtained as

$$V^{\rm F} = \frac{8\sqrt{2}\pi(m\mu)^{3/2}}{3\hbar^3} + \frac{16384\sqrt{2}\pi m^{15/2}\mu^{11/2}J^2}{15015\hbar^3} \tag{121}$$

up to the second order in J. It is independent of the spin s.

There is no ℓth order spin-Drude conductivity for all $\ell \geqslant 6$. It is straightforward to see that there is no spin conductivity for $\ell = 0, 1, 2, 3, 4$. We calculate the nonlinear spin-dependent conductivity for $\ell = 5$. Because

$$\frac{\partial^6\varepsilon_s}{\partial k_x^2\partial k_y^4} = \frac{\partial^6\varepsilon_s}{\partial k_y^2\partial k_z^4} = \frac{\partial^6\varepsilon_s}{\partial k_z^2\partial k_x^4} = -\frac{\partial^6\varepsilon_s}{\partial k_x^4\partial k_y^2} = -\frac{\partial^6\varepsilon_s}{\partial k_y^4\partial k_z^2} = -\frac{\partial^6\varepsilon_s}{\partial k_z^4\partial k_x^2} = 48sJ, \tag{122}$$

we obtain

$$\sigma_{\rm spin}^{yyyx;x} = 48\frac{(e/\hbar)^6}{(i\omega + 1/\tau)^5}V^{\rm F}J \tag{123}$$

and similar ones arising from Eq. (122). We conclude that there is only fifth-order nonlinear spin-Drude conductivity.

The tight-binding model corresponding to the continuum model (87) is given by

$$H = \frac{\hbar^2}{ma^2}(3 - \cos ak_x - \cos ak_y - \cos ak_z)\sigma_0 + 8J\sigma_z(\cos ak_y - \cos ak_x)(\cos ak_z - \cos ak_y) \times (\cos ak_x - \cos ak_z), \tag{124}$$

which is defined on the cubic lattice. The Fermi surface is shown in Fig. 1(f2).

XV. DISCUSSION

We studied the higher-order nonlinear spin-Drude conductivity in higher-wave symmetric magnets characterized by the number of nodes. We found that the system having $(\ell + 1)$ nodes has only ℓth order nonlinear spin-Drude conductivity. It is highly contrasted to the usual system [16], where various higher-order contributions are present. Especially, only third-order nonlinear conductivity is present in g-wave altermagnets and only fifth-order nonlinear conductivity is present in i-wave altermgnets. The prominent feature is that f-wave magnets in two dimensions generate the perfect nonreciprocal spin current because there is only second-order nonlinear spin current.

These results are derived from two-band models, where the pseudospin degrees of freedom are absent, and only a certain order of the nonlinear spin current is generated. However, there are systems involving the pseudospin degrees of freedom, where the Hamiltonian is not diagonal in general. The study of such systems is a future problem.

The d-wave magnet in two dimensions is realized in organic materials [4], perovskite materials [6], and twisted magnetic van der Waals bilayers [46]. The d-wave altermagnet in three dimensions is realized in RuO_2 [47–51], Mn_5Si_3 [52], and $FeSb_2$ [53]. A g-wave altermagnet is realized in twisted magnetic van der Waals bilayers [46]. The Fermi surface splitting of the g-wave altermagnet in three dimensions is experimentally observed in MnTe [54–58] and CrSb [59–63]. An i-wave altermagnet in two dimensions is realized in twisted magnetic van der Waals bilayers [46]. It was theoretically proposed that CeNiAsO is a p-wave magnet [10]. Our paper could motivate further search on materialization of higher-wave symmetric magnets.

We estimate the magnitude of electric field. The dimensionless electric field is given by $E/(\frac{\hbar k}{e\tau})$ with

$$\frac{\hbar k}{e\tau} = 6.6 \times 10^5 [\mathrm{kgm/As^3}], \tag{125}$$

where we have used the relaxation time [64,65] $\tau = 3.4 \times 10^{-12}$s and the typical momentum [54] $k = 0.35$ Å^{-1}. The experimental value of the electric field [66] is $E = 1[\mathrm{V/\mu m}] = 10^6\,[\mathrm{kgm/As^3}]$. It is possible to apply a larger electric field [67] $E = 10[\mathrm{V/\mu m}]$ satisfying $E/(\frac{\hbar k}{e\tau}) > 1$, where the higher-order nonlinear conductivity is significantly large. High-efficiency spin-current generation proportional to E^ℓ is possible in them if we apply an electric field larger than $E = 6.6 \times 10^5[\mathrm{kgm/As^3}]$.

ACKNOWLEDGMENTS

The author is very much grateful to M. Hirschberger for helpful discussions on the subject. This work is supported by CREST, JST (Grant No. JPMJCR20T2), and Grants-in-Aid for Scientific Research from MEXT KAKENHI (Grant No. 23H00171).

[1] M. I. D'Yakonov and V. I. Perel', Possibility of orientating electron spins with current, J. Expt. Theor. Phys. Lett. **13**, 467 (1971).

[2] M. I. Dyakonov and V. I. Perel, Current-induced spin orientation of electrons in semiconductors, Phys. Lett. A **35**, 459 (1971).

[3] J. Sinova, S. O. Valenzuela, J. Wunderlich, C. H. Back, and T. Jungwirth, Spin Hall effects, Rev. Mod. Phys. **87**, 1213 (2015).

[4] M. Naka, S. Hayami, H. Kusunose, Y. Yanagi, Y. Motome, and H. Seo, Spin current generation in organic antiferromagnets, Nat. Commun. **10**, 4305 (2019).

[5] R. Gonzalez-Hernandez, L. Šmejkal, K. Vborn, Y. Yahagi, J. Sinova, T. Jungwirth, and J. Železn, Efficient electrical spin splitter based on nonrelativistic collinear antiferromagnetism, Phys. Rev. Lett. **126**, 127701 (2021).

[6] M. Naka, Y. Motome, and H. Seo, Perovskite as a spin current generator, Phys. Rev. B **103**, 125114 (2021).

[7] A. Bose, N. J. Schreiber, R. Jain, D.-F. Shao, H. P. Nair, J. Sun, X. S. Zhang, D. A. Muller, E. Y. Tsymbal, D. G. Schlom, and D. C. Ralph, Tilted spin current generated by the collinear antiferromagnet ruthenium dioxide, Nat. Electron. **5**, 267 (2022).

[8] M. Naka, Y. Motome, and H. Seo, Altermagnetic perovskites, arXiv:2411.11025.

[9] S. Hayami, Y. Yanagi, and H. Kusunose, Momentum-dependent spin splitting by collinear antiferromagnetic ordering, J. Phys. Soc. Jpn. **88**, 123702 (2019).

[10] A. B. Hellenes, T. Jungwirth, J. Sinova, and L. Šmejkal, Unconventional p-wave magnets, arXiv:2309.01607.

[11] T. Jungwirth, R. M. Fernandes, E. Fradkin, A. H. MacDonald, J. Sinova, and L. Smejkal, From supefluid ^{3}He to altermagnets, arXiv:2411.00717.

[12] L. Šmejkal, J. Sinova, and T. Jungwirth, Beyond conventional ferromagnetism and antiferromagnetism: A phase with nonrelativistic spin and crystal rotation symmetry, Phys. Rev. X **12**, 031042 (2022).

[13] L. Šmejkal, J. Sinova, and T. Jungwirth, Emerging research landscape of altermagnetism, Phys. Rev. X **12**, 040501 (2022).

[14] Y. Gao, S. A. Yang, and Q. Niu, Field induced positional shift of Bloch electrons and its dynamical implications, Phys. Rev. Lett. **112**, 166601 (2014).

[15] I. Sodemann and L. Fu, Quantum nonlinear Hall effect induced by Berry curvature dipole in time-reversal invariant materials, Phys. Rev. Lett. **115**, 216806 (2015).

[16] T. Ideue, K. Hamamoto, S. Koshikawa, M. Ezawa, S. Shimizu, Y. Kaneko, Y. Tokura, N. Nagaosa, and Y. Iwasa, Bulk rectification effect in a polar semiconductor, Nat. Phys. **13**, 578 (2017).

[17] H. Liu, J. Zhao, Y.-X. Huang, W. Wu, X.-L. Sheng, C. Xiao, and S. A. Yang, Intrinsic second-order anomalous Hall effect and its application in compensated antiferromagnets, Phys. Rev. Lett. **127**, 277202 (2021).

[18] Y. Michishita and N. Nagaosa, Dissipation and geometry in nonlinear quantum transports of multiband electronic systems, Phys. Rev. B **106**, 125114 (2022).

[19] H. Watanabe and Y. Yanase, Nonlinear electric transport in odd-parity magnetic multipole systems: Application to Mn-based compounds, Phys. Rev. Res. **2**, 043081 (2020).

[20] C. Wang, Y. Gao, and D. Xiao, Intrinsic nonlinear Hall effect in antiferromagnetic tetragonal CuMnAs, Phys. Rev. Lett. **127**, 277201 (2021).

[21] R. Oiwa and H. Kusunose, Systematic analysis method for nonlinear response tensors, J. Phys. Soc. Jpn. **91**, 014701 (2022).

[22] A. Gao, Y.-F. Liu, J.-X. Qiu, B. Ghosh, T. V. Trevisan, Y. Onishi, C. Hu, T. Qian, H.-J. Tien, S.-W. Chen *et al.*, Quantum metric nonlinear Hall effect in a topological antiferromagnetic heterostructure, Science **381**, 181 (2023).

[23] N. Wang, D. Kaplan, Z. Zhang, T. Holder, N. Cao, A. Wang, X. Zhou, F. Zhou, Z. Jiang, C. Zhang *et al.*, Quantum metric-induced nonlinear transport in a topological antiferromagnet, Nature (London) **621**, 487 (2023).

[24] K. Das, S. Lahiri, R. B. Atencia, D. Culcer, and A. Agarwal, Intrinsic nonlinear conductivities induced by the quantum metric, Phys. Rev. B **108**, L201405 (2023).

[25] D. Kaplan, T. Holder, and B. Yan, Unification of nonlinear anomalous Hall effect and nonreciprocal magnetoresistance in metals by the quantum geometry, Phys. Rev. Lett. **132**, 026301 (2024).

[26] Y. D. Wang, Z. F. Zhang, Z.-G. Zhu, and G. Su, Intrinsic nonlinear Ohmic current, Phys. Rev. B **109**, 085419 (2024).

[27] L. Xiang, B. Wang, Y. Wei, Z. Qiao, and J. Wang, Linear displacement current solely driven by the quantum metric, Phys. Rev. B **109**, 115121 (2024).

[28] Z.-H. Gong, Z. Z. Du, H.-P. Sun, H.-Z. Lu, and X. C. Xie, Nonlinear transport theory at the order of quantum metric, arXiv:2410.04995v2.

[29] K. Hamamoto, M. Ezawa, K. W. Kim, T. Morimoto, and N. Nagaosa, Nonlinear spin current generation in noncentrosymmetric spin-orbit coupled systems, Phys. Rev. B **95**, 224430 (2017).

[30] M. Kameda, D. Hirobe, S. Daimon, Y. Shiomi, S. Takahashi, and E. Saitoh, Microscopic formulation of nonlinear spin current induced by spin pumping, J. Magn. Magn. Mater. **476**, 459 (2019).

[31] S. Hayami, M. Yatsushiro, and H. Kusunose, Nonlinear spin Hall effect in PT-symmetric collinear magnets, Phys. Rev. B **106**, 024405 (2022).

[32] S. Hayami, Linear and nonlinear spin-current generation in polar collinear antiferromagnets without relativistic spin-orbit coupling, Phys. Rev. B **109**, 214431 (2024).

[33] D. Kaplan, T. Holder, and B. Yan, Unifying semiclassics and quantum perturbation theory at nonlinear order, SciPost Phys. **14**, 082 (2023).

[34] Y. Fang, J. Cano, and Sayed Ali Akbar Ghorashi, Quantum geometry induced nonlinear transport in altermagnets, Phys. Rev. Lett. **133**, 106701 (2024).

[35] S. Okumura, T. Morimoto, Y. Kato, and Y. Motome, Quadratic optical responses in a chiral magnet, Phys. Rev. B **104**, L180407 (2021).

[36] K. Maeda, B. Lu, K. Yada, and Y. Tanaka, Theory of tunneling spectroscopy in *p*-wave altermagnet-superconductor hybrid structures, J. Phys. Soc. Jpn. **93**, 114703 (2024).

[37] M. Ezawa, Topological insulators based on *p*-wave altermagnets; Electrical control and detection of the altermagnetic domain wall, Phys. Rev. B **110**, 165429 (2024).

[38] B. Brekke, P. Sukhachov, H. G. Giil, A. Brataas, and J. Linder, Minimal models and transport properties of unconventional *p*-wave magnets, Phys. Rev. Lett. **133**, 236703 (2024).

[39] M. Ezawa, Purely electrical detection of the Neel vector of p-wave magnets based on linear and nonlinear conductivities, arXiv:2410.21854.

[40] L. Šmejkal, A. H. MacDonald, J. Sinova, S. Nakatsuji, and T. Jungwirth, Anomalous Hall antiferromagnets, Nat. Rev. Mater. **7**, 482 (2022).

[41] D. Zhu, Z.-Y. Zhuang, Z. Wu, and Z. Yan, Topological superconductivity in two-dimensional altermagnetic metals, Phys. Rev. B **108**, 184505 (2023).

[42] Sayed Ali Akbar Ghorashi, T. L. Hughes, and J. Cano, Altermagnetic routes to Majorana modes in zero net magnetization, Phys. Rev. Lett. **133**, 106601 (2024).

[43] Y.-X. Li and C.-C. Liu, Majorana corner modes and tunable patterns in an altermagnet heterostructure, Phys. Rev. B **108**, 205410 (2023).

[44] M. Ezawa, Detecting the Neel vector of altermagnets in heterostructures with a topological insulator and a crystalline valley-edge insulator, Phys. Rev. B **109**, 245306 (2024).

[45] M. Ezawa, Intrinsic nonlinear conductivity induced by quantum geometry in altermagnets and measurement of the in-plane Neel vector, arXiv:2409.09241.

[46] Y. Liu, J. Yu, and C.-C. Liu, Twisted magnetic van der Waals bilayers: An ideal platform for altermagnetism, Phys. Rev. Lett. **133**, 206702 (2024).

[47] K.-H. Ahn, A. Hariki, K.-W. Lee, and J. Kunes, Antiferromagnetism in RuO_2 as *d*-wave Pomeranchuk instability, Phys. Rev. B **99**, 184432 (2019).

[48] L. Šmejkal, R. Gonzalez-Hernandez, T. Jungwirth, and J. Sinova, Crystal time-reversal symmetry breaking and spontaneous Hall effect in collinear antiferromagnets, Sci. Adv. **6**, eaaz8809 (2020).

[49] T. Tschirner, P. Keler, R. D. G. Betancourt, T. Kotte, D. Kriegner, B. Buechner, J. Dufouleur, M. Kamp, V. Jovic, L. Smejkal, J. Sinova, R. Claessen, T. Jungwirth, S. Moser, H. Reichlova, and L. Veyrat, Saturation of the anomalous Hall effect at high magnetic fields in altermagnetic RuO_2, APL Mater. **11**, 101103 (2023).

[50] O. Fedchenko, J. Minar, A. Akashdeep, S. W. D'Souza, D. Vasilyev, O. Tkach, L. Odenbreit, Q. L. Nguyen, D. Kutnyakhov, N. Wind, L. Wenthaus, M. Scholz, K. Rossnagel, M. Hoesch, M. Aeschlimann, B. Stadtmueller, M. Klaeui, G. Schoenhense, G. Jakob, T. Jungwirth *et al.*, Observation of time-reversal symmetry breaking in the band structure of altermagnetic RuO_2, Sci. Adv. **10**, eadj4883 (2024).

[51] Z. Lin, D. Chen, W. Lu, X. Liang, S. Feng, K. Yamagami, J. Osiecki, M. Leandersson, B. Thiagarajan, J. Liu, C. Felser, and J. Ma, Observation of giant spin splitting and *d*-wave spin texture in room temperature altermagnet RuO_2, arXiv:2402.04995.

[52] M. Leiviskä, J. Rial, A. Badura, R. L. Seeger, I. Kounta, S. Beckert, D. Kriegner, I. Joumard, E. Schmoranzerova, J. Sinova, O. Gomonay, A. Thomas, S. T. B. Goennenwein, H. Reichlova, L. Smejkal, L. Michez, T. Jungwirth, and V. Baltz, Anisotropy of the anomalous Hall effect in the altermagnet candidate Mn_5Si_3 films, Phys. Rev. B **109**, 224430 (2024).

[53] I. I. Mazin, K. Koepernik, M. D. Johannes, R. Gonzalez-Herndez, and L. Šmejkal, Prediction of unconventional magnetism in doped $FeSb_2$, Proc. Natl. Acad. Sci. **118**, e2108924118 (2021).

[54] J. Krempaský, L. Šmejkal, S. W. D'Souza, M. Hajlaoui, G. Springholz, K. U. F. Alarab, P. C. Constantinou, V. Strocov, D. Usanov, W. R. Pudelko, R. Gonzez-Herndez, A. B. Hellenes, Z. Jansa, H. Reichlov, Z. Šob, R. D. G. Betancourt, P. Wadley, J. Sinova, D. Kriegner, J. Min, J. H. Dil, and T. Jungwirth, Altermagnetic lifting of Kramers spin degeneracy, Nature (London) **626**, 517 (2024).

[55] S. Lee, S. Lee, S. Jung, J. Jung, D. Kim, Y. Lee, B. Seok, J. Kim, B. G. Park, L. Šmejkal, C.-J. Kang, and C. Kim, Broken Kramers degeneracy in altermagnetic MnTe, Phys. Rev. Lett. **132**, 036702 (2024).

[56] T. Osumi, S. Souma, T. Aoyama, K. Yamauchi, A. Honma, K. Nakayama, T. Takahashi, K. Ohgushi, and T. Sato, Observation of a giant band splitting in altermagnetic MnTe, Phys. Rev. B **109**, 115102 (2024).

[57] M. Hajlaoui, S. W. D'Souza, L. Šmejkal, D. Kriegner, G. Krizman, T. Zakusylo, N. Olszowska, O. Caha, J. Michalička, A. Marmodoro, K. Vyborny, A. Ernst, M. Cinchetti, J. Minar, T. Jungwirth, and G. Springholz, Temperature dependence of relativistic valence band splitting induced by an altermagnetic phase transition, Adv. Mater. **36**, 2314076 (2024).

[58] Z. Liu, M. Ozeki, S. Asai, S. Itoh, and T. Masuda, Chiral split magnon in altermagnetic MnTe, Phys. Rev. Lett. **133**, 156702 (2024).

[59] S. Reimers, L. Odenbreit, L. Šmejkal, V. N. Strocov, P. Constantinou, A. B. Hellenes, R. J. Ubiergo, W. H. Campos, V. K. Bharadwaj, A. Chakraborty, T. Denneulin, W. Shi, R. E. Dunin-Borkowski, S. Das, M. Kli, J. Sinova, and M. Jourdan, Direct observation of altermagnetic band splitting in CrSb thin films, Nat. Commun. **15**, 2116 (2024).

[60] G. Yang, Z. Li, S. Yang, J. Li, H. Zheng, W. Zhu, Z. Pan, Y. Xu, S. Cao, W. Zhao, A. Jana, J. Zhang, M. Ye, Y. Song, L.-H. Hu, L. Yang, J. Fujii, I. Vobornik, M. Shi, H. Yuan *et al.*, Three-dimensional mapping and electronic origin of large altermagnetic splitting near Fermi level in CrSb, Nat. Commun. **16**, 1442 (2025).

[61] J. Ding, Z. Jiang, X. Chen, Z. Tao, Z. Liu, J. Liu, T. Li, J. Liu, Y. Yang, R. Zhang, L. Deng, W. Jing, Y. Huang, Y. Shi, S. Qiao, Y. Wang, Y. Guo, D. Feng, and D. Shen, Large band-splitting in *g*-wave type altermagnet CrSb, Phys. Rev. Lett. **133**, 206401 (2024).

[62] C. Li, M. Hu, Z. Li, Y. Wang, W. Chen, B. Thiagarajan, M. Leandersson, C. Polley, T. Kim, Hui Liu, C. Fulga, M. G. Vergniory, O. Janson, O. Tjernberg, and J. van den Brink, Topological Weyl altermagnetism in CrSb, arXiv:2405.14777.

[63] W. Lu, S. Feng, Y. Wang, D. Chen, Z. Lin, Xin Liang, S. Liu, W. Feng, K. Yamagami, J. Liu, Claudia Felser, Q. Wu, and J.

Ma, Observation of surface Fermi arcs in altermagnetic Weyl semimetal CrSb, arXiv:2407.13497.

[64] M. Trama, V. Cataudella, C. A. Perroni, F. Romeo, and R. Citro, Tunable spin and orbital Edelstein effect at (111) $LaAlO_3/SrTiO_3$ interface, Nanomaterials **12**, 2494 (2022).

[65] Z. Z. Du, C. M. Wang, S. Li, Hai-Zhou Lu, and X. C. Xie, Disorder-induced nonlinear Hall effect with time-reversal symmetry, Nat. Commun. **10**, 3047 (2019).

[66] G. Sala, M. T. Mercaldo, K. Domi, S. Gariglio, M. Cuoco, C. Ortix, and A. D. Caviglia, The quantum metric of electrons with spin-momentum locking, arXiv:2407.06659.

[67] P. He, H. Isobe, G. K. W. Koon, J. Y. Tan, J. Hu, J. Li, N. Nagaosa, and J. Shen, Third-order nonlinear Hall effect in a quantum Hall system, Nat. Nanotechnol. **19**, 1460 (2024).